


RESEARCH

Open Access



Preparation and characterization of cellulose nanocrystal extracted from *Calotropis procera* biomass

Kaili Song^{1,2,3*} , Xiaoji Zhu^{1,3}, Weiming Zhu^{1,3} and Xiaoyan Li^{4*}

Abstract

Calotropis procera fiber (CPF) is the fruit fiber of *C. procera* and belongs to a typical cellulosic fiber. In this study, *Calotropis procera* fiber (CPF) was first purified in the pretreatment process including delignification and bleaching before the isolation of cellulose nanocrystal. Chemical composition of *Calotropis procera* fiber was determined according to TAPPI standard method. It was composed of 64.0 wt% cellulose, 19.5 wt% hemicelluloses, and 9.7 wt% of lignin. The morphology of the *Calotropis procera* fiber and fiber after each pretreatment process was also investigated. Cellulose nanocrystal was extracted by classical sulfuric acid hydrolysis of the pretreated *Calotropis procera* fiber. TEM and SEM were used to analyze the morphologies of the obtained CNC. The crystallinity, thermal stability and suspension stability of the CNC were also investigated. The interesting results proved that this under-utilized biomass could be exploited as a new source of cellulose raw material for the production of cellulose nanocrystal.

Keywords: Cellulose nanocrystals, *Calotropis procera* fiber, Agriculture residue, Acid hydrolysis

Introduction

Calotropis procera fiber (CPF) is the fruit fiber of *C. procera* that can be collected from its mature fruits with 3–4.5 in. long and 2–2.5 in. wide. This fruit fiber belongs to a typical cellulosic fiber but has been overlooked for centuries (Kanchan and Atreya 2016; Tarabi et al. 2016; Zheng et al. 2016). Recently, *Calotropis procera* fiber has received more attention in the textile industry and for potential application in fiber-reinforced composites. The fiber possesses thin cell wall, large lumen and low density; thus, it exhibits excellent insulation property against sound and heat. In addition, this fiber could be used in making ropes, carpets, or sewing threads. It has been reported that the cellulose content of this fiber was in the range of 60–75%; thus, it could be a potential cellulosic

material to produce cellulose nanocrystal (Kanchan and Atreya 2016).

Cellulose nanocrystal (CNC), a kind of nanomaterial derived from cellulose, possessed lots of desirable property, like extremely outstanding mechanical strength, biocompatible and biodegradable, high specific surface area and so on (Yu et al. 2013; Li et al. 2016). The distinctive property of cellulose nanocrystals make it useful building block in various applications, for instance as reinforcing agents (Ye et al. 2015; Song et al. 2017, 2020), biomedical implant (Rueda et al. 2013), rheological modifier (Li et al. 2015), nanocomposites (Yu et al. 2014) as well as electronic components (Eyley et al. 2012).

Currently, cellulose nanocrystal can be obtained from wood, non-wood fibers, algae, tunicates, and agro-industrial residue or biomass. However, cellulosic agro-industrial residue or biomass are the most promising sources because of their low cost and availability (Reddy and Yang 2011; Zhang et al. 2012; Chen et al. 2013). During the pursuit of naturally abundant, renewable and sustainable cellulosic raw materials, lots of researches have already been focused on the utilization of agricultural residues or biomass for the extraction of cellulose nanocrystal,

*Correspondence: kailisong12@163.com; xiaoyanli89@hebust.edu.cn

¹ Engineering Research Center for Eco-Dyeing and Finishing of Textiles, College of Materials and Textiles, Zhejiang Sci-Tech University, Hangzhou 310018, Zhejiang, China

⁴ College of Textile and Garment, Hebei University of Science and Technology, Hebei 050018, China

Full list of author information is available at the end of the article

such as rice straw (Johar et al. 2012; Hsieh 2013), grape skins (Lu and Hsieh 2012), pineapple leaf (Dos Santos et al. 2013), sugarcane bagasse (De Moraes Teixeira et al. 2011), banana rachis (Elanthikkal et al. 2010) and so on. *Calotropis procera* fiber could be exploited as a suitable new cellulosic material for the production of cellulose nanocrystal.

This study was to isolate cellulose from *Calotropis procera* fiber and investigate the effect of treatment on the properties of the obtained cellulose nanocrystal. The pretreatment process was carried out to remove those impurities on *Calotropis procera* fiber, such as the wax, lignin and make cellulose more accessible to chemicals. It is the first time that systematical study of pretreatment and acid hydrolysis of *Calotropis procera* fiber for cellulose nanocrystal extraction was conducted. The influence of pretreatment on the chemical composition and morphology of *Calotropis procera* fiber was investigated and characterized. The morphology, crystallinity and thermal stability of the obtained cellulose nanocrystal were also investigated.

Materials and methods

Materials

Calotropis procera fiber as raw cellulose materials was kindly supplied by World Agroforestry Centre, Kunming institute of Botany, CAS. Acetic acid and hydrochloride acid were purchased from Sinopharm Chemical Reagent Co., Ltd. (Beijing, China). Sulfuric acid was purchased from Pinghu Chemical Reagent Co., Ltd (Pinghu, China). All the chemicals used in this research were of analytical grade and applied without further purification.

Determination of the chemical composition of *Calotropis procera* fiber

The chemical compositions of *Calotropis procera* fiber (CPF) and the fiber after each treatment were determined according to Technical Association of the Pulp and Paper Industry (TAPPI) standard. The lignin content was determined according to the TAPPI norm T222 om-88 (de Oliveira et al. 2016; Espino et al. 2014). Briefly, 1 g of CPF was added into the 15-mL H₂SO₄ solution (72 wt%), and maintained at room temperature for 2 h. Then, the distilled water, 560 mL, was added and boiled the mixture for 4 h before the centrifuge to get the insoluble lignin. The obtained lignin was oven-dried and weighted. The lignin quantity was determined using Eq. (1).

$$\text{Lignin (\%)} = \frac{M_1}{M} \times 100, \quad (1)$$

where M_1 was the obtained lignin mass, M was the initial sample mass.

Hemicellulose content was determined according to the TAPPI T257 om-09. Holocellulose content was quantified with sodium chlorite treatment according to the reported procedure (dos Santos et al. 2013). Fiber, 1 g, was added into the solution, 30 mL, containing acetic acid 0.25 mL, sodium chlorite 0.3 g and kept at 75 °C for 1 h. The mixture is then cooled down and the residue is filtered and washed thoroughly with water. The residue was finally dried and weighted. The holocellulose content was calculated using Eq. (2).

$$\text{Holocellulose (\%)} = \frac{M_2}{M} \times 100, \quad (2)$$

where M_2 was the obtained residue mass, M was the initial sample mass.

Cellulose content was determined by extracting holocellulose with the aqueous sodium hydroxide (17.5%) for 5 h before quenching the reaction with ice. The obtained white powder was washed with copious amount of water until filtrate becoming neutral (Xu and Hanna 2010). The cellulose content was calculated using Eq. (3).

$$\text{Cellulose (\%)} = \frac{M_3}{M} \times 100,$$

where M_3 was the obtained white powder mass, M was the initial sample mass.

Pretreatment of *Calotropis procera* fiber

Calotropis procera fiber (CPF) was first washed and dried. The pretreatment process of CPF included alkali treatment, delignification and bleaching treatment (Ray et al. 2001; Neto et al. 2013). Firstly, the cleaned CPF, 1 g, was immersed in NaOH solution (2 wt%), 100 mL, at room temperature and stirred for 3 h to finish the alkali treatment to remove the impurities including pectin, wax. The alkali-treated fiber was washed thoroughly till neutral. The delignification process was carried out with dewaxed CPF, 1 g, suspended in acetic acid (93% v/v), 50 mL, and hydrochloride acid solution (0.3% v/v) under strong stirring for 3 h at 90 °C and then washed till neutral pH value. The bleaching procedure was performed by adding the obtained delignified CPF into the mixture of H₂O₂ (5 wt%) and NaOH (3.8 wt%) at a ratio of 1:50 and stirred at room temperature for 3 h before washing thoroughly.

Extraction of cellulose nanocrystal

Cellulose nanocrystal (CNC) was obtained by sulfuric acid hydrolysis according to the reported method (Lin et al. 2012). The pretreated CPF powder, 1 g, was slowly added into H₂SO₄ solution (63 wt%), 30 mL, under vigorously stirring at room temperature for 1 h. After that, the hydrolysis was quenching by adding iced water, 300 mL,

into the mixture. The resultant mixture was first centrifuged at 1000 rpm for 10 min to remove large particles, and then centrifuged at 11,000 rpm for 15 min to obtain cellulose nanocrystal. The obtained cellulose nanocrystal was washed and centrifuged repeatedly for 3 times before dialysis against distilled water for 2 days. The obtained CNC was processed by ultrasonic processor (VCX 500:500 W, Sonics & Materials, Newton, CT) to suspension better before further application.

Particle size and zeta potential measurement of the obtained cellulose nanocrystal

The particle size and zeta potential of the obtained CNC were measured by Nano-Z5 Analyzer (Malvern Instruments Co., Ltd., UK). The obtained CNC suspension was diluted to 0.1–0.6 wt% concentration firstly. Then, the suspension was put into a container for measurement.

Morphology analysis

Morphologies of the obtained CNC were measured by Hitachi S-4800 field emission scanning electron microscope (Hitachi Co., Ltd., Japan). CNC powder was obtained by freeze drying of CNC suspension and the powder was sputter coating with a layer of gold firstly before SEM analysis. Also, TEM analysis was carried out for morphology measurement. The obtained CNC suspension was diluted to 1–4 mg/mL concentration before

deposited into copper grid. TEM analysis was carried out at 100 kV. The diameter and length distribution of the obtained CNC was analysis using Image J software (National Institutes of Health Co., Ltd., USA).

Characterization of the obtained cellulose nanocrystal

FTIR analysis of the obtained CNC was performed by Nicolet 6700 spectrometer (Thermo Fisher Scientific, USA) using KBr pellet methods. TG analysis of CNC was performed by TGA-50 thermal stability analyzer at a heating rate of 15 °C/min form room temperature to 600 °C using N₂ atmosphere. The crystallinity index of the obtained CNC was analyzed by Bruker D4 X-ray diffractometer. The measurement was carried out at 40 kV under Cu Kα radiation. CrI of the samples was calculated by Eq. (3) (Mariano et al. 2016).

$$CrI = \frac{I_{002} - I_{am}}{I_{002}} \times 100, \tag{3}$$

where I_{002} was the intensity of 200 peak (I_{200}) between $2\theta = 22\text{--}23^\circ$ and I_{am} was the minimum intensity between the peaks at 200 and 110 (I_{am}) $2\theta = 18\text{--}19^\circ$.

Results and discussion

Pretreatment of *Calotropis procera* fiber

The preparation process to isolate CNC from *Calotropis procera* fiber (CPF) is illustrated in Fig. 1. The first step

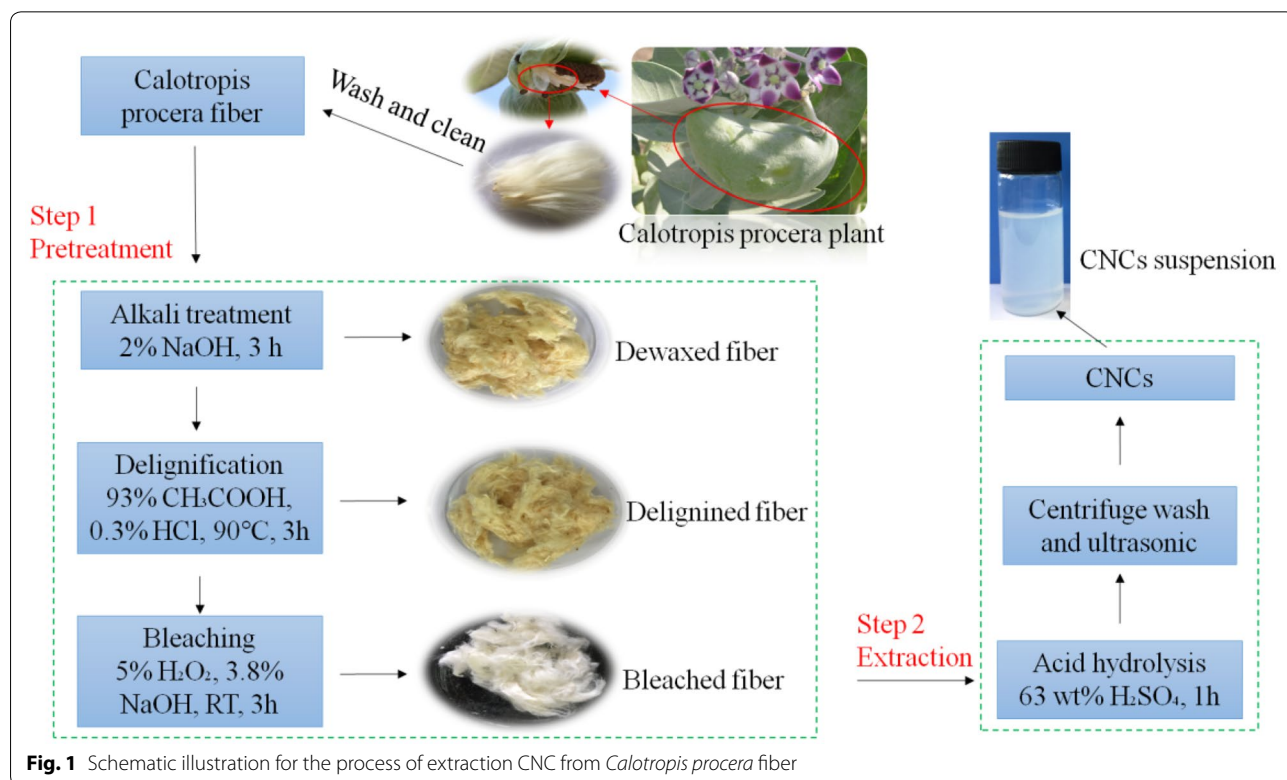


Fig. 1 Schematic illustration for the process of extraction CNC from *Calotropis procera* fiber

was to isolate cellulose from the obtained natural plant fiber by removing lignin, hemicellulose and other impurities. As shown in Table 1, the original *Calotropis procera* fiber consisted of 64.1 wt% cellulose, 19.5 wt% hemicellulose, 9.7 wt% lignin. The cellulose content of *Calotropis procera* fiber is much higher than other reported agricultural biomass, such as 50.7 wt% for kenaf, 61.0 wt% for fiber flax, 41.1 wt% for onion skin (Rhim et al. 2015), which proved that *Calotropis procera* fiber could be proposed as a novel and abundant feedstock for nanocellulose production. After alkali treatment, the extractives such as pectin and wax were removed without significant affect the lignin, hemicellulose and cellulose content of the fiber. Almost 83% of lignin was removed after delignification as shown in Table 1. The cellulose content was found to be 91.3 wt% after bleaching treatment. In addition, the content of lignin and hemicellulose was also partly reduced as the result of bleaching. Various radicals (HO·, O₂·, and perhydroxyl anions HOO⁻) were produced during bleaching and those radicals could destroy

the chromophore of lignin (Lee et al. 2009), and further resulted the degradation of lignin and hemicelluloses.

The morphology of the original *Calotropis procera* fiber after treatment is shown in Fig. 2. From Fig. 2a, b, it can be seen that the original CPF exhibited smooth surface. There is no obvious difference in the appearance of the fiber surface except that lots of tiny wrinkles formed after the removal of wax and other extractives. After the delignification (Fig. 2e, f), the surface of the treated fiber became rough and lots of wrinkles were formed. The bleaching process could further promote the removal of the lignin and hemicelluloses from CPF and resulted in a rough and coarse fiber morphology as shown in Fig. 2g, h.

Figure 3 shows the FTIR spectra of the original and pretreated *Calotropis procera* fibers. The peaks around 3340 cm⁻¹ and 2907 cm⁻¹ were assigned to O–H stretch and C–H stretch stretching of aliphatic moieties in polysaccharides. In the spectra of CPF, the band at 1732 cm⁻¹ was assigned to the ester linkage of carboxylic group of ferulic and *p*-coumaric acids of lignin; the peak at 1502 cm⁻¹ was assigned to the C=C stretching of aromatic rings of lignin. The sharp peak appearing at 1640 cm⁻¹ in all samples was attributed to the bending mode of absorbed water in cellulose. The peaks at 1163 cm⁻¹ and 899 cm⁻¹ were associated with the C–O stretching and C–H vibrations of hemicellulose. The presence of those peaks confirmed the existence of lignin and hemicellulose in CPF. However, the absorption band at 1732 cm⁻¹ and 1502 cm⁻¹ disappeared in the delignified fiber, suggesting that lignin was successfully removed during this process. Additionally, in the

Table 1 Chemical composition of *Calotropis procera* fiber and selected common natural fibers

Constituent (%)	Lignin	Cellulose	Hemicellulose
Original fiber	9.7 ± 1.2	64.1 ± 1.6	19.5 ± 1.2
Alkali treated fiber	9.5 ± 1.3	64.1 ± 1.4	20.1 ± 0.8
Delignified fiber	1.7 ± 0.9	74.5 ± 0.5	24.1 ± 1.1
Bleached fiber	0.4 ± 0.1	91.3 ± 1.1	8.2 ± 0.9
Kenaf	15.8 ± 1.9	50.7 ± 1.1	21.5 ± 1.5
Fiber flax	2.2 ± 0.5	61.0 ± 0.9	18.6 ± 1.5
Onion skin	38.9 ± 1.3	41.1 ± 1.1	16.2 ± 0.6

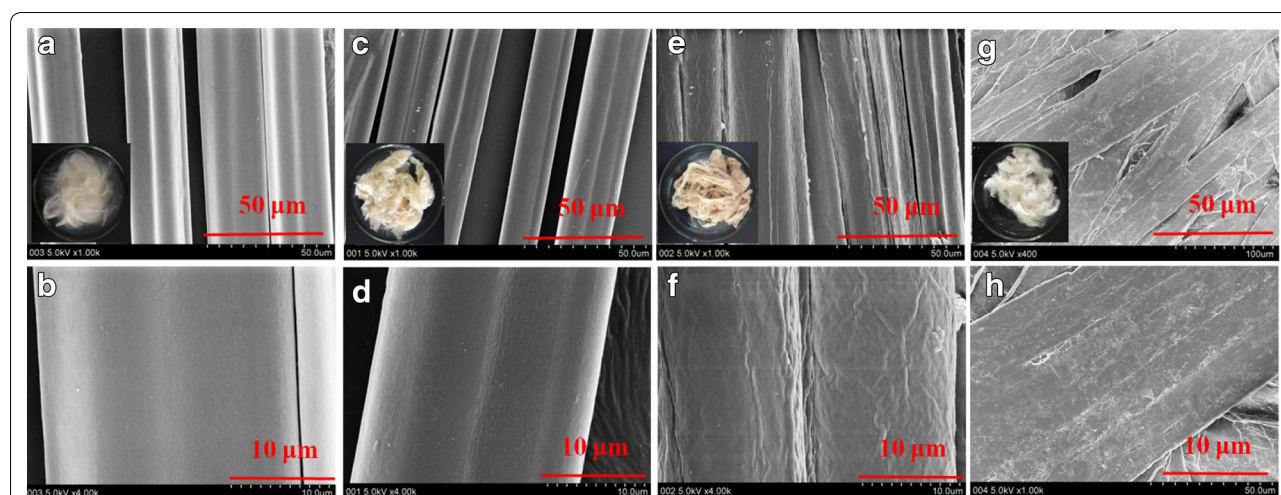
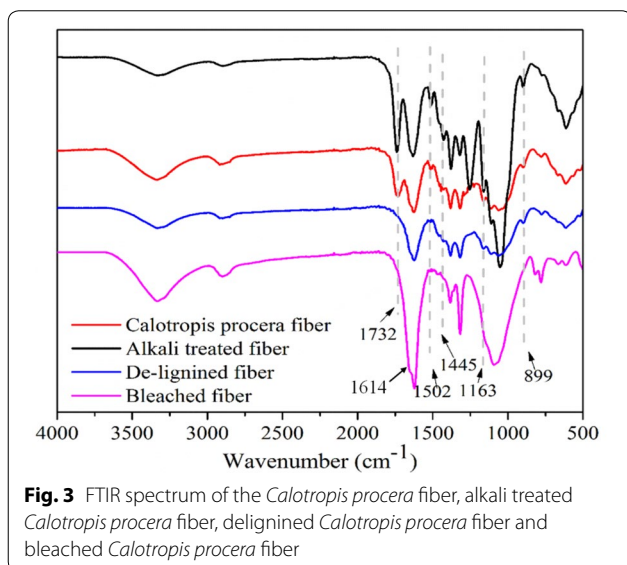


Fig. 2 Morphology of **a, b** the *Calotropis procera* fiber; **c, d** dewaxed *Calotropis procera* fiber; **e, f** *Calotropis procera* fiber after the delignification; **g, h** *Calotropis procera* fiber after bleaching

Table 2 Onset temperature (T_{onset}), degradation temperature on maximum weight-loss rate (T_{max}), weight loss (W_L) for CPF and the obtained CNC

Samples	Cellulose thermal degradation			Carbonic residue degradation		
	T_{onset} (°C)	T_{max} (°C)	W_L (%)	T_{onset} (°C)	T_{max} (°C)	W_L (%)
Calotropis procera fiber	277	330	79	420	510	31
Obtained CNC	180	205	57	367	406	43



bleached fiber, the disappearance of the band at 899 cm^{-1} confirmed the removal of hemicellulose.

Extraction of cellulose nanocrystal

TEM graphs of the obtained CNC are shown in Fig. 4a. As can be seen, CNC showed uniform needle-like shape with 250-nm length and 12-nm diameter, which was similar with the reported works (dos Santos et al. 2013; Rhim et al. 2015; An et al. 2016). From Fig. 4d, e, we could also see the needle-like cellulose nanocrystal. Figure 4b, c show the diameter and length distributions of the obtained CNC. It could be seen that the length of the obtained CNC was ranging from 100 to 400 nm and diameter between 4 and 12 nm. Polydispersity of the obtained CNC was 0.39 (measured by dynamic light scattering), which was lower than the reported literature (4.1 for CNC obtained from filter paper and 0.49 for spherical cellulose nanocrystals).

The dispersion stability of the nanocrystal in different polar solvent is an important parameter to evaluate dispersity of CNC as nanofillers in manufacturing nanocomposites. The dispersibility of CNC strongly depends on their surface functionalization, aspect ratio, and surface charges. The obtained CNC was ultrasonicated and

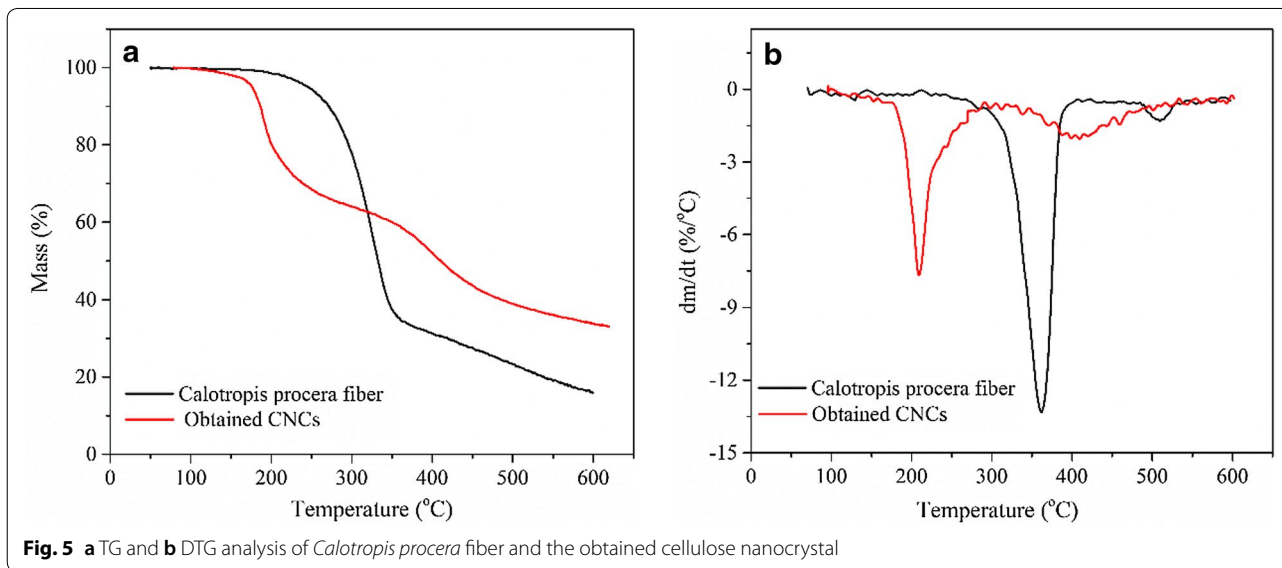
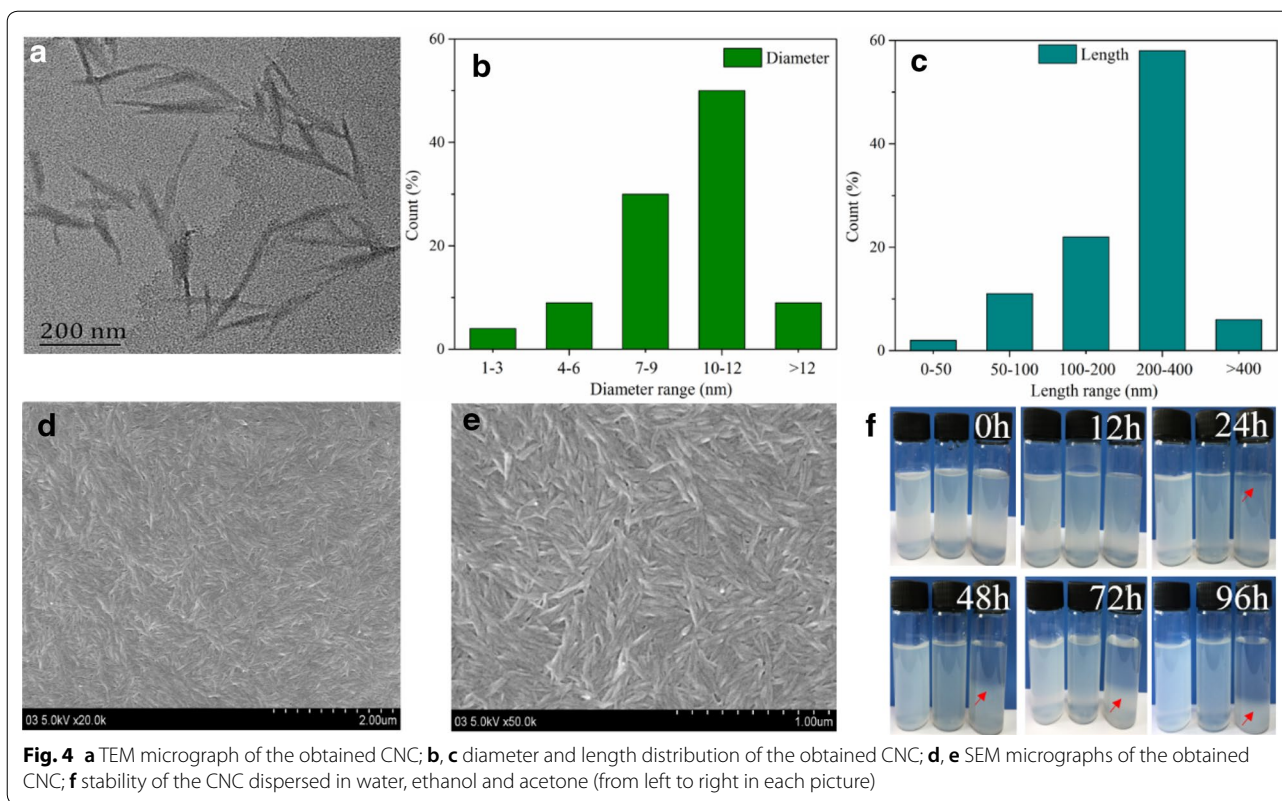
dispersed in water, ethanol and acetone at a concentration of 10 mg/mL to compare its colloidal stability. As shown in Fig. 4f, the nanocrystal dispersed in water and ethanol stay stable even after 96 h, which showed that the obtained CNC was completely dispersed. After hydrolysis, negatively charged sulfate group was introduced onto CNC, which contributed to the stabilization of CNC suspension by repulsive forces. However, CNC dispersed in acetone solvent started to separate after 24 h due to the fact that CNC tends to highly agglomerate in acetone solvent.

Thermal analysis

Thermal stability of CPF and the obtained CNC was investigated. Their corresponding thermogram is presented in Fig. 5 and the corresponding degradation temperature is summarized in Table 2. From Fig. 5, we can see that CPF showed a weight loss from 300 to 400 °C, which could be due to the decomposition of the glycosyl units in cellulose fiber (Chen et al. 2012; Vinayaka et al. 2017). As for the obtained CNC, it showed a lower degradation temperature which could be attributed to the introduced sulfate groups on the nanocrystal surface. The first degradation step basically corresponding to the cellulose degradation process was between 160 and 250 °C and the second degradation step was attributed to the oxidation and breakdown of the charred residue to lower molecular weight gaseous products. The introduction of sulfate groups at cellulose nanocrystal could accelerate the depolymerization of cellulose (Camarero Espinosa et al. 2013). Also, the reported degradation temperature of CNC from Soy hulls and Flax was 170 °C and 186 °C (Neto et al. 2013).

XRD and FTIR analysis

XRD analysis of the obtained CNC is shown in Fig. 6a. The XRD diagrams of *Calotropis procera* fiber and the obtained CNC showed peaks at $2\theta = 16.0^\circ$, and 22.1° , which could be attributed to the cellulose I characteristic peaks. Crystallinity index (CrI) of the materials is summarized in Table 3. The Crystallinity index of the obtained CNC showed a significant increase compared with *Calotropis procera* fiber, indicating that the acid digested the amorphous hemicelluloses and the defective



regions in *Calotropis procera* fiber. The crystallinity of the obtained CNC was similar with the reported literature as listed in Table 3 (Zhao et al. 2015, 2016; Neto et al. 2013; Johar et al. 2012).

The FTIR spectra of the original *Calotropis procera* fiber and the obtained cellulose nanocrystal are shown in Fig. 6b. The absence of peaks around 1742 cm^{-1} and 1522 cm^{-1} at cellulose nanocrystal was due to the removal of lignin after the pretreatment of *Calotropis procera* fiber. The new peak at 1205 cm^{-1} was resulted

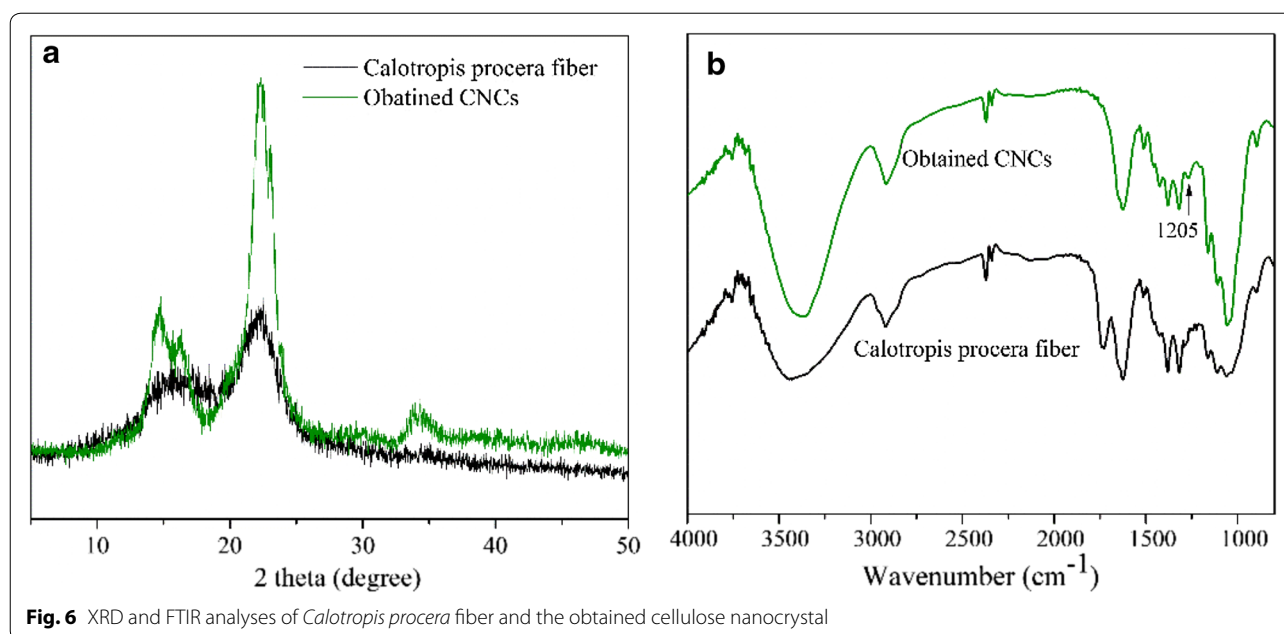


Fig. 6 XRD and FTIR analyses of *Calotropis procera* fiber and the obtained cellulose nanocrystal

Table 3 The crystallinity index (Crl) of the obtained CNC in this study and comparing with the reported literature

Materials	Extraction method	Crl (%)	References
CNC from this study	Acid hydrolysis	68.7	This study
<i>Calotropis procera</i> fiber	–	30.1	This study
CNC from Soy hulls	Acid hydrolysis	71.5	Neto et al. (2013)
CNC from Pine	Acid hydrolysis	56.0	Zhao et al. (2015)
CNC from corn husk	Acid hydrolysis	70.7	Zhao et al. (2015)
CNC from rice husk	Acid hydrolysis	59.0	Johar et al. (2012)

from the introduced sulfate groups by sulfuric acid hydrolysis.

Conclusion

Cellulose nanocrystal can be isolated from *Calotropis procera* fiber, an under-utilized agriculture biomass. The cellulose content of the *Calotropis procera* fiber was 64.1%. The chemical pretreatment which removed the non-cellulosic constituents of *Calotropis procera* fiber was found to be an essential and fundamental procedure for the isolation of cellulose nanocrystal. The obtained CNC exhibited a needle-like shape with an average diameter and length of 12 nm and 250 nm, leading to an aspect ratio of approximately 30. The crystallinity index of the obtained CNC was 68.7%. Furthermore, the obtained CNC showed good thermal stability. The CNC obtained from the biomass, *Calotropis procera* fiber, showed great potential as reinforcement agents during the manufacturing of renewable

nanocomposites due to their relatively high aspect ratio and high crystallinity.

Abbreviation

CNC: cellulose nanocrystals.

Acknowledgements

Not applicable.

Authors' contributions

KS is involved in collecting, reviewing the literature and performing the preparation of the CNC. WZ is involved in the characterization of the materials. XL is involved in guiding the analysis, improving and revising the manuscript. Both the authors are involved in writing the manuscript. All authors read and approved the final manuscript.

Funding

This work was financially supported by the public projects of Zhejiang Province (LGF20E030005, LGF20E030006), Zhejiang Provincial Top Key Academic Discipline of Chemical Engineering and Technology of Zhejiang Sci-Tech University (CETT 2017003), the Opening Project of Key Laboratory of Clean Dyeing and Finishing Technology of Zhejiang Province (Project Number: 1808) and Scientific Research Foundation of Zhejiang Sci-Tech University (Grant Number 18012211-Y).

Ethics approval and consent to participate

Not applicable.

Consent for publication

Not applicable.

Competing interests

The authors declare that they have no competing interests.

Author details

¹ Engineering Research Center for Eco-Dyeing and Finishing of Textiles, College of Materials and Textiles, Zhejiang Sci-Tech University, Hangzhou 310018, Zhejiang, China. ² Key Laboratory of Clean Dyeing and Finishing Technology of Zhejiang Province, Shaoxing University, Shaoxing 312000, Zhejiang, China. ³ Key Laboratory of Advanced Textile Materials and Manufacturing Technology,

Ministry of Education, Zhejiang Sci-Tech University, Hangzhou 310018, Zhejiang, China. ⁴ College of Textile and Garment, Hebei University of Science and Technology, Hebei 050018, China.

Received: 6 September 2019 Accepted: 15 November 2019

Published online: 22 November 2019

References

- An X, Wen Y, Cheng D (2016) Preparation of cellulose nano-crystals through a sequential process of cellulase pretreatment and acid hydrolysis. *Cellulose* 23:2409–2420. <https://doi.org/10.1007/s10570-016-0964-4>
- Camarero Espinosa S, Kuhnt T, Foster EJ, Weder C (2013) Isolation of thermally stable cellulose nanocrystals by phosphoric acid hydrolysis. *Biomacromolecules* 14:1223–1230. <https://doi.org/10.1021/bm400219u>
- Chen L, Reddy N, Wu X, Yang Y (2012) Thermoplastic films from wheat proteins. *Ind Crops Prod* 35:70–76. <https://doi.org/10.1016/j.indcrop.2011.06.009>
- Chen L, Reddy N, Yang Y (2013) Remediation of environmental pollution by substituting poly(vinyl alcohol) with biodegradable warp size from wheat gluten. *Environ Sci Technol* 47:4505–4511. <https://doi.org/10.1021/es304429s>
- de Moraes Teixeira E, Bondancia TJ, Teodoro KBR (2011) Sugarcane bagasse whiskers: extraction and characterizations. *Ind Crops Prod* 33:63–66. <https://doi.org/10.1016/j.indcrop.2010.08.009>
- de Oliveira FB, Bras J, Pimenta MTB (2016) Production of cellulose nanocrystals from sugarcane bagasse fibers and pith. *Ind Crops Prod* 93:48–57. <https://doi.org/10.1016/j.indcrop.2016.04.064>
- dos Santos RM, Neto WPF, Silvério HA (2013) Cellulose nanocrystals from pineapple leaf, a new approach for the reuse of this agro-waste. *Ind Crops Prod* 50:707–714. <https://doi.org/10.1016/j.indcrop.2013.08.049>
- Elanthikkal S, Gopalakrishnanpanicker U, Varghese S, Guthrie JT (2010) Cellulose microfibrils produced from banana plant wastes: isolation and characterization. *Carbohydr Polym* 80:852–859. <https://doi.org/10.1016/j.carbpol.2009.12.043>
- Espino E, Cakir M, Domenek S (2014) Isolation and characterization of cellulose nanocrystals from industrial by-products of *Agave tequilana* and barley. *Ind Crops Prod* 62:552–559. <https://doi.org/10.1016/j.indcrop.2014.09.017>
- Eyley S, Shariki S, Dale SEC (2012) Ferrocene-decorated nanocrystalline cellulose with charge carrier mobility. *Langmuir* 28:6514–6519. <https://doi.org/10.1021/la3001224>
- Hsieh YL (2013) Cellulose nanocrystals and self-assembled nanostructures from cotton, rice straw and grape skin: a source perspective. *J Mater Sci* 48:7837–7846. <https://doi.org/10.1007/s10853-013-7512-5>
- Johar N, Ahmad I, Dufresne A (2012) Extraction, preparation and characterization of cellulose fibres and nanocrystals from rice husk. *Ind Crops Prod* 37:93–99. <https://doi.org/10.1016/j.indcrop.2011.12.016>
- Kanchan T, Atreya A (2016) *Calotropis gigantea*. *Wilderness Environ Med* 27:350–351. <https://doi.org/10.1016/j.wem.2015.12.011>
- Lee YJ, Chung CH, Day DF (2009) Sugarcane bagasse oxidation using a combination of hypochlorite and peroxide. *Bioresour Technol* 100:935–941. <https://doi.org/10.1016/j.biortech.2008.06.043>
- Li MC, Wu Q, Song K (2015) Cellulose nanoparticles as modifiers for rheology and fluid loss in bentonite water-based fluids. *ACS Appl Mater Interfaces* 7:5009–5016. <https://doi.org/10.1021/acsami.5b00498>
- Li Y, Liu Y, Chen W (2016) Facile extraction of cellulose nanocrystals from wood using ethanol and peroxide solvothermal pretreatment followed by ultrasonic nanofibrillation. *Green Chem* 18:1010–1018. <https://doi.org/10.1039/C5GC02576A>
- Lin N, Bruzzone C, Dufresne A (2012) TEMPO-oxidized nanocellulose participating as crosslinking aid for alginate-based sponges. *ACS Appl Mater Interfaces* 4:4948–4959. <https://doi.org/10.1021/am301325r>
- Lu P, Hsieh YL (2012) Cellulose isolation and core-shell nanostructures of cellulose nanocrystals from chardonnay grape skins. *Carbohydr Polym* 87:2546–2553. <https://doi.org/10.1016/j.carbpol.2011.11.023>
- Mariano M, Cervená R, Soldi V (2016) Thermal characterization of cellulose nanocrystals isolated from sisal fibers using acid hydrolysis. *Ind Crops Prod* 94:454–462. <https://doi.org/10.1016/j.indcrop.2016.09.011>
- Neto WPF, Silvério HA, Dantas NO, Pasquini D (2013) Extraction and characterization of cellulose nanocrystals from agro-industrial residue—Soy hulls. *Ind Crops Prod* 42:480–488. <https://doi.org/10.1016/j.indcrop.2012.06.041>
- Ray D, Sarkar BK, Rana AK, Bose NR (2001) Mechanical properties of vinyl ester resin matrix composites reinforced with alkali-treated jute fibres. *Compos Part A Appl Sci Manuf* 32:119–127. [https://doi.org/10.1016/S1359-835X\(00\)00101-9](https://doi.org/10.1016/S1359-835X(00)00101-9)
- Reddy N, Yang Y (2011) Completely biodegradable soyprotein-jute biocomposites developed using water without any chemicals as plasticizer. *Ind Crops Prod* 33:35–41. <https://doi.org/10.1016/j.indcrop.2010.08.007>
- Rhim JW, Reddy JP, Luo X (2015) Isolation of cellulose nanocrystals from onion skin and their utilization for the preparation of agar-based bio-nanocomposites films. *Cellulose* 22:407–420. <https://doi.org/10.1007/s10570-014-0517-7>
- Rueda L, Saralegi A, Fernández-d'Arlas B (2013) In situ polymerization and characterization of elastomeric polyurethane-cellulose nanocrystal nanocomposites. *Cell response evaluation*. *Cellulose* 20:1819–1828. <https://doi.org/10.1007/s10570-013-9960-0>
- Song K, Xu H, Xu L (2017) Preparation of cellulose nanocrystal-reinforced keratin bioadsorbent for highly effective and recyclable removal of dyes from aqueous solution. *Bioresour Technol* 232:254–262. <https://doi.org/10.1016/j.biortech.2017.01.070>
- Song K, Zhu W, Li X, Yu Z (2020) A novel mechanical robust, self-healing and shape memory hydrogel based on PVA reinforced by cellulose nanocrystal. *Mater Lett* 260:126884
- Tarabi N, Mousazadeh H, Jafari A, Taghizadeh-Tameh J (2016) Evaluation of properties of bast fiber extracted from *Calotropis* (Millkweed) by a new decorticator machine and manual methods. *Ind Crops Prod* 83:545–550. <https://doi.org/10.1016/j.indcrop.2015.12.071>
- Vinayaka DL, Guna V, Madhavi D, Arpitha M, Reddy N (2017) *Ricinus communis* plant residues as a source for natural cellulose fibers potentially exploitable in polymer composites. *Ind Crops Prod* 100:126–131. <https://doi.org/10.1016/j.indcrop.2017.02.019>
- Xu Y, Hanna MA (2010) Optimum conditions for dilute acid hydrolysis of hemicellulose in dried distillers grains with solubles. *Ind Crops Prod* 32:511–517. <https://doi.org/10.1016/j.indcrop.2010.06.024>
- Ye C, Malak ST, Hu K (2015) Cellulose nanocrystal microcapsules as tunable cages for nano- and microparticles. *ACS Nano* 9:10887–10895. <https://doi.org/10.1021/acs.nano.5b03905>
- Yu H, Qin Z, Liang B (2013) Facile extraction of thermally stable cellulose nanocrystals with a high yield of 93% through hydrochloric acid hydrolysis under hydrothermal conditions. *J Mater Chem A* 1:3938–3944. <https://doi.org/10.1039/c3ta01150j>
- Yu H-Y, Qin Z-Y, Yan C-F, Yao J-M (2014) Green nanocomposites based on functionalized cellulose nanocrystals: a study on the relationship between interfacial interaction and property enhancement. *ACS Sustain Chem Eng* 2:875–886. <https://doi.org/10.1021/sc400499g>
- Zhang S, Keshwani DR, Xu Y, Hanna MA (2012) Alkali combined extrusion pretreatment of corn stover to enhance enzyme saccharification. *Ind Crops Prod* 37:352–357. <https://doi.org/10.1016/j.indcrop.2011.12.001>
- Zhao Y, Zhao Y, Yang Y (2015) Modified soy protein to substitute non-degradable petrochemicals for slashing industry. *Ind Crops Prod* 67:466–474. <https://doi.org/10.1016/j.indcrop.2015.01.058>
- Zheng Y, Cao E, Zhu Y (2016) Perfluorosilane treated *Calotropis gigantea* fiber: instant hydrophobic-oleophilic surface with efficient oil-absorbing performance. *Chem Eng J* 295:477–483. <https://doi.org/10.1016/j.cej.2016.03.074>

Publisher's Note

Springer Nature remains neutral with regard to jurisdictional claims in published maps and institutional affiliations.